Looper Optimal Multivariable Control for Hot Strip Finishing Mill*

*By Kenya FUKUSHIMA,** Yuichi TSUJI,** Shinji UENO,** Yoshiharu ANBE,*** Kunio SEKIGUCHI*** and Yoshiro SEKI****

Synopsis

A looper optimal multivariable control system based on an optimal regulator theory has been developed. Goal of controlling the hot strip finishing mill loopers is to stabilize rolling operation and to maintain product quality by controlling the tension applied to the strip and the looper angle within their reference values.

The most difficult problem in looper control is to achieve simultaneously the interfering tension control and looper angle control. In recent years, a non-interactive control employing cross-controllers has been adopted and brought a dramatic increase in control accuracy, although the response time is limited. Thus, a new method with improved response time is desirable.

In this paper, a looper optimal multivariable control based on the optimal regulator theory employing a looper drive system with speed control loop is proposed. Other topics discussed includes the results of an investigation of simplifying the control system by the use of a programmable controller. In addition, it is demonstrated that the optimal multivariable control is effective compared with the conventional control and the non-interactive control as employed in the hot strip finishing mill of Hirohata Works of Nippon Steel Corporation.

Key words: process control; hot rolling; hot strip mill; looper control; optimal regulator theory.

I. Introduction

Loopers located between stands in a hot strip finishing mill perform at least two important functions:

(1) Preventing the changes in width and thickness of a strip by regulating the interstand tension at a desired value.

(2) Preventing the formation of strip loop between stands and providing stable rolling operation by maintaining the looper angle at a desired value.

Additional disturbance to the looper system is caused by the increasing use of low-temperature heating of slabs, high-carbon steels and high-speed rolling. Moreover, the demand for high dimensional precision such as the thickness, width and crown of strip has been strongly requested. Therefore, it is important to develop a high-performance looper control.

The most tenacious problem in looper control is to achieve the simultaneous control of looper angle and tension, which interact with each other. The conventional looper control includes:

1) Tension control which involves controlling the current of the looper motor and thus indirectly maintaining the tension at the reference value.
2) Looper angle control which involves maintaining the looper angle at the desired value by regulating the rotating speed of main motor.

However, sufficient precision has not been achieved with the conventional control due to the difficulty of reducing mutual interaction and the effects of a resonant system within the looper system.

In order to overcome this difficulty, a non-interactive control system employing cross-controllers has been installed in the looper system. The non-interactive control has greatly improved the precision in control of tension and looper angle. One problem of this system, however, was to maintain good response and thus control accuracy of looper angle control and tension control in the presence of large disturbances sich as encountered during the rolling of thin strips. It was for this reason that looper optimal multivariable control employing a tension-absorbing function provided by changing the looper angle was adopted.

In this paper, the looper optimal multivariable control based on an integra-type optimal regulator employing a looper drive system with speed control loop is proposed. Other topics discussed include results of an investigation of simplifying the control system to enable use of a programmable logic controller. In addition, it will be demonstrated that the optimal multivariable control is effective compared with the conventional control and the non-interactive control employed in an actual plant.

II. Overview of Facility

A simplified configuration diagram[1] of the hot strip finishing mill of Hirohata Works of Nippon Steel Corporation is shown in Fig. 1. The finishing mill is composed of six stands four high mill. The loopers are installed between the stands. The mill has the following characteristics:

(1) All of the motors are controlled by digital speed controllers.

(2) A hydraulic screw down is installed to each stand and hydraulic automatic gage control (AGC) is introduced.

(3) Low-inertia motors are employed as the looper drive system. Since the motors are connected directly to the loopers without gears, this system has lower inertia than conventional systems. The optimal multivariable control has been applied to the last (No. 5) looper.

---

* Partly published in *Transactions of The Institute of Electrical Engineers of Japan*, **108-c** (1988), 31, in Japanese. Manuscript received on September 3, 1987; accepted in the final form on January 14, 1988.

** Equipment Department, Hirohata Works, Nippon Steel Corporation, Fuji-cho, Hirohata-ku, Himeji 671-11.

*** Heavy Apparatus Engineering Laboratory, Fuchu Works, Toshiba Corporation, Toshiba-cho, Fuchu 183.

III. Development of Looper Control

1. Conventional Looper Control

The configuration for conventional looper control[2] is shown in Fig. 2. The looper motor current reference calculation controller (CRCC) calculates the current reference that should be output by the looper drive system based on the reference value for tension on the strip. The current reference is then sent to the current controller of the looper motor. Next, the looper height controller (LHC) calculates the speed correction value of the main motor from the looper angle deviation between the reference looper angle and the actual looper angle. This value is then sent to the main motor speed controller, where it is used to bring the looper angle to the reference value.

The conventional control needs no sensor for measuring the strip tension. However, this method of control has the following faults.

(1) It is difficult to attain the tension reference value due to acceleration and deceleration of the looper motor.

(2) Since the mutual interaction between the looper angle and the tension forms a resonant system, it is difficult to improve looper angle control performance.

2. Looper Non-interactive Control

In the looper non-interactive control,[3] the looper angle and tension are controlled in a non-interactive manner that permits improved stability and response time. In addition, the control accuracy of the tension is increased, since an actually measured tension value is employed for feedback control.

The configuration of non-interactive control is given in Fig. 3. The controller comprises main controllers (LTC: looper tension controller; and LHC: looper height controller) and cross-controllers. The cross-controllers compensate the interference between looper angle and tension. The transfer functions of

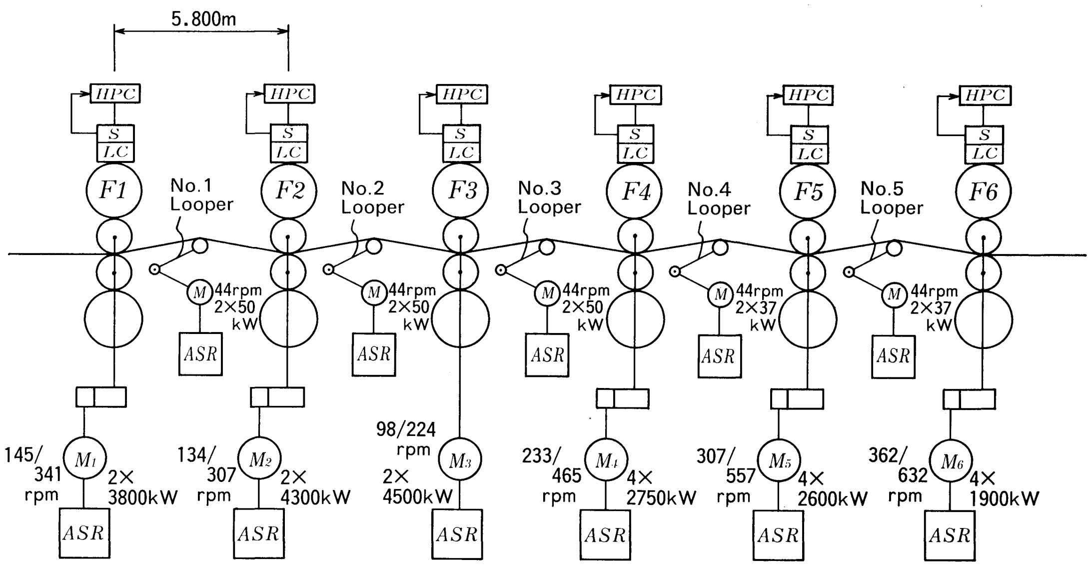

HPC: Hydraulic gap controller
S: Roll gap detector
ASR: Automatic speed regulator
LC: Load cell

Fig. 1. Configuration of hot strip finishing mill.

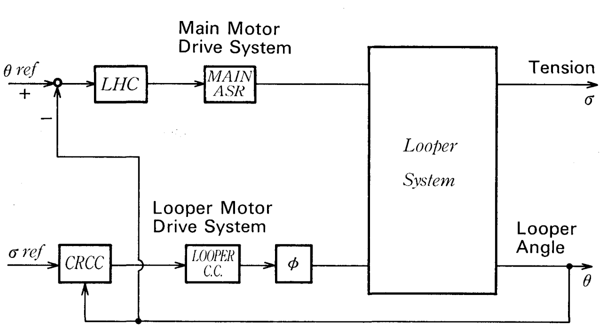

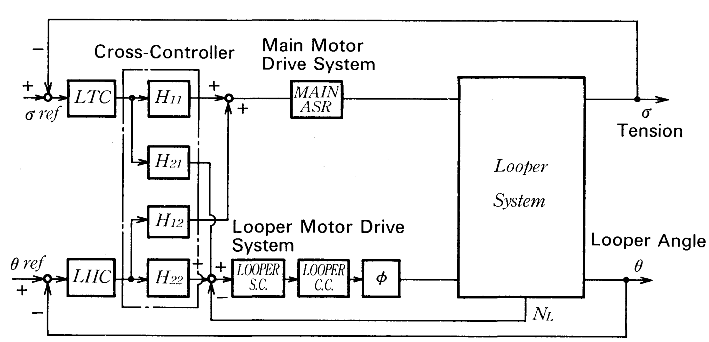

(Symbols)
σ : Tension
θ : Looper Angle
LHC : Looper Height Control
MAIN ASR : Main Motor Drive System
φ : Torque factor
LTC : Looper Tension Control
CRCC : Current Reference Calculation Controller
C.C. : Current Controller
S.C : Speed Controller
S : Laplacian
ref : Reference

Fig. 2. Block diagram of conventional control.

Fig. 3. Block diagram of non-interactive control.

the cross-controllers are as follows:

$$H_{11}=1,\ H_{22}=1\ , \quad \cdots\cdots(1)$$

$$H_{12}=\frac{F_3(\theta)\cdot T_{21}\cdot s\cdot(1+T_{23}\cdot s)}{(1+T_{22}\cdot s)(1+T_{30}\cdot s)\{K_{10}+(L/E)s\}}\ , \quad \cdots\cdots(2)$$

$$H_{21}=\frac{F_2(\theta)\cdot(1/\eta_L)\cdot(1+T_{30}\cdot s)(1+T_{22}\cdot s)}{J_L\cdot T_{21}\cdot s^2\cdot(1+T_{23}\cdot s)+(1+T_{22}\cdot s)}\ , \quad \cdots\cdots(3)$$

where, T_{21}, T_{22}, T_{23}, T_{30}, K_{10}, L, E: constants
$F_2(\theta)$, $F_3(\theta)$: functions
J_L: looper inertia
s: Laplacien.

The looper tension controller (LTC) and the looper height controller (LHC) both act as proportional and integral (PI) controllers. They output the main motor speed correction value and looper motor speed correction value.

Non-interactive control has led to a remarkable improvement in response time and stability over the conventional control method. However, the following problems still remain:

(1) Though the non-interactive control is performed, the response of the tension control system is affected by the response of the main motor speed controller. Thus, the desired performance can not be achieved.

(2) Due to the limitations of response time in the tension control system, some types of operations involving large disturbances can not be performed. Tension fluctuations due to disturbances causes problems in product quality and operability.

IV. Development of Looper Optimal Multivariable Control

1. Configuration of Looper Optimal Multivariable Control[4)]

The looper drive system is shown in Fig. 4. Application of the optimal regulator to the looper system is necessary to linearize the object system. When the speed control of looper is employed, the overall system is divided into three independent sub-systems as indicated in Fig. 5:

1) Tension generating system,
2) Main motor speed control system, and,
3) Looper drive system and looper mechanisms.

Modeling is then performed by creating state equations for each of the three sub-systems.

The controlled variables are the tension stress (σ) and the looper angle (θ). The manipulated variables are the speed correction value of the upstream stand main motor ($\Delta N_{M,ref}$) and the speed correction value of the looper motor ($\Delta N_{L,ref}$).

1. Tension Generation System

The state equations of the tension generation system are given as

$$\begin{cases}\dot{x}_t=A_t\cdot x_t+B_t\cdot u_t-E_t\cdot\omega_t\ ,\\ y_t=x_s\ ,\end{cases} \quad \cdots\cdots(4)$$

where, A_t, B_t, E_t: the index matrices
x_t, u_t, y_t: the vectors representing a deviation from the normal state
ω_t: the disturbance vector.

Each of the elements is:

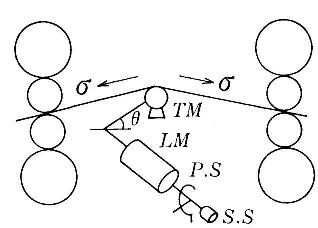

TM: Tension meter LM: Looper drive motor
PS: Position sensor SS: Speed sensor
θ: Looper angle σ: Tension

Fig. 4. Looper driving system.

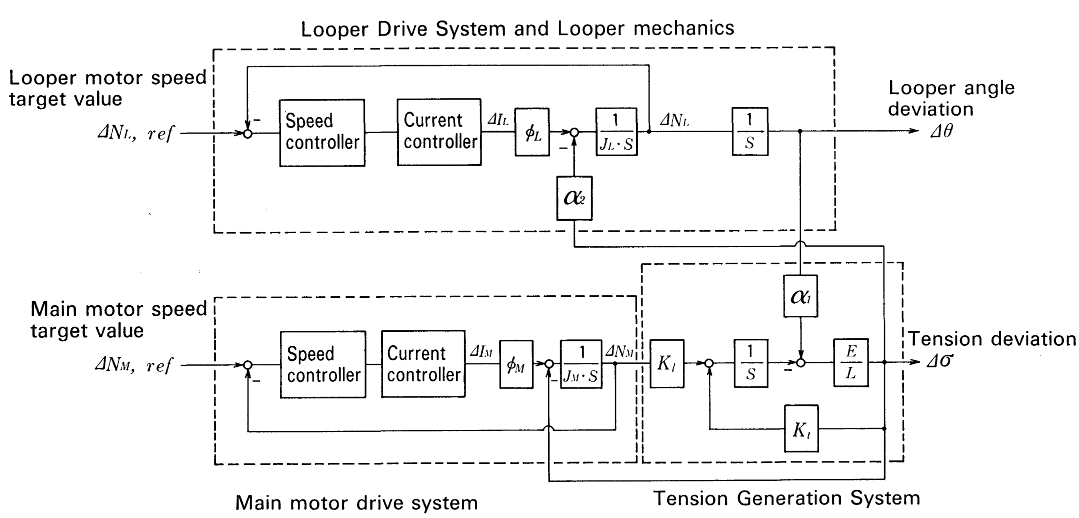

α_1, α_2: The interaction parameter
J_M, J_L: The inertia of main and looper motor, respectively
L: The length of strip between stands
ϕ_M, ϕ_L: The torque coefficient of main and looper motor, respectively
E: Young's modulus of strip
K_l, K_t: Constants

Fig. 5. Block diagram of looper system.

$$\begin{cases} x_t \triangleq \Delta\sigma, \\ u_t \triangleq [\Delta N_M, \Delta\theta]^T, \\ y_t \triangleq \Delta\sigma. \end{cases} \quad \cdots\cdots(5)$$

Here, $\Delta\sigma$: the deviation of tension stress
$\Delta\theta$: the looper angle
ΔN_M: the revolution of main motor
T: transposition.

2. Main Motor Speed Control System

The state equations of the main motor speed control system are given by

$$\begin{cases} \dot{x}_m = A_m \cdot x_m + B_m \cdot u_m + E_m \cdot \omega_m, \\ y_m = C_m \cdot x_m, \end{cases} \quad \cdots\cdots(6)$$

where, A_m, B_m, C_m, E_m: the index matrices
x_m, u_m, y_m: the vectors representing a deviation from the normal state
ω_m: the disturbance vector.

Each of the elements is:

$$\begin{cases} x_m \triangleq [\Delta I_M, \Delta N_M, x_{m3}, x_{m4}, x_{m5}, x_{m6}]^T, \\ u_m \triangleq [\Delta N_{M,ref}, \Delta\sigma]^T, \\ y_m \triangleq \Delta N_M. \end{cases} \quad \cdots\cdots(7)$$

Here, ΔI_M: the current deviation of main motor
$x_{m3} \sim x_{m6}$: the state variables of speed controller of the main motor.

3. Looper Drive System and Looper Mechanisms

The state equations of the looper drive system and looper mechanisms are given by

$$\begin{cases} \dot{x}_h = A_h \cdot x_h + B_h \cdot u_h + E_h \cdot \omega_h, \\ y_h = C_h \cdot x_h, \end{cases} \quad \cdots\cdots(8)$$

where, A_h, B_h, C_h, E_h: the index matrices
x_h, u_h, y_h: the vectors representing a deviation from the normal state
ω_h: the disturbance vector.

Each of the elements is:

$$\begin{cases} x_h \triangleq [\Delta I_L, \Delta N_L, \Delta\theta, x_{h4}, x_{h5}, x_{h6}, x_{h7}]^T, \\ u_h \triangleq [\Delta N_{L,ref}, \Delta\sigma]^T, \\ y_h \triangleq \Delta\theta. \end{cases} \quad \cdots\cdots(9)$$

Here, ΔI_L: the armature current deviation of looper motor
ΔN_L: the revolution deviation of looper motor
$x_{h4} \sim x_{h7}$: the state variables of the speed controller of the looper motor.

By combination of these three sub-systems, a complete model of the looper system can be achieved. However, this model requires the use of 14 state variables and is too complex to apply in actual use. Due to the number of sensors required for the speed controllers of the main motors and the looper motors, x_{m3} through x_{m6} and x_{h4} through x_{h7} are the state vectors to be omitted. The modified state equations employed in the present system are given by Eqs. (10) to (13).

$$\begin{cases} \dot{x} = A \cdot x + B \cdot u, \\ y = C \cdot x, \end{cases} \quad \cdots\cdots(10)$$

where, $x \triangleq [\Delta I_M, \Delta N_M, \Delta\sigma, \Delta I_L, \Delta N_L, \Delta\theta]^T$, $\cdots\cdots(11)$
$u \triangleq [\Delta N_{M,ref}, \Delta N_{L,ref}]^T$, $\cdots\cdots(12)$
$y \triangleq [\Delta\sigma, \Delta\theta]^T$. $\cdots\cdots(13)$

Furthermore an integral-type optimal regulator is included as an additional integrated term to eliminate the difference between controlled variable and reference value. The control system configuration is shown in Fig. 6. The manipulated vector for the looper system is derived as a sum of the state feedback vector and the main controller output vector: the manipulated vector u is given by

$$u = K_I \int_{t_0}^{t} (y_R - y)dt + F \cdot x + Z_{(t_0)}. \quad \cdots\cdots(14)$$

Here, F: the state feedback gain matrix
K_I: the main controller gain matrix
t: the time
Y_R: the reference value vector
$Z(t_0)$: the manipulated variable at $t = t_0$.

Rearrangement in terms of the state vector $\tilde{u}$ and the manipulated vector $\tilde{x}$ leads to

$$\begin{cases} \tilde{x} = [(y_R - y)^T, \dot{x}^T]^T, \\ \tilde{u} = \dot{u}. \end{cases} \quad \cdots\cdots(15)$$

In turn, the state equation can be described to the following equation by replacing for $\tilde{u}$ and $\tilde{x}$:

$$\dot{\tilde{x}} = \tilde{A} \cdot \tilde{x} + \tilde{B} \cdot \tilde{u}. \quad \cdots\cdots(16)$$

The terms, $\tilde{A}$ and $\tilde{B}$, are the matrices of the expanded state equation. In this situation, the value $\tilde{u}$ to minimize the performance index (17) is given by Eq. (18).

$$J = \int_0^\infty (\tilde{x}^T Q \tilde{x} + \tilde{u}^T R \tilde{u}) dt \quad \cdots\cdots(17)$$

$$\tilde{u} = -R^{-1} \cdot \tilde{B}^T \cdot K \cdot \tilde{x} \quad \cdots\cdots(18)$$

The positive matrices, Q and R, are the weight matrices, and the matrix K is the correct solution of the Riccati equation:

$$K\tilde{A} + \tilde{A}^T K - K\tilde{B}R^{-1}\tilde{B}^T K + Q = 0. \quad \cdots\cdots(19)$$

If the matrix K is taken as

$$K = \begin{bmatrix} \overbrace{K_{11}}^{2} & \overbrace{K_{12}}^{6} \\ K_{21} & K_{22} \end{bmatrix} \begin{matrix} \}2 \\ \}6 \end{matrix} \quad \cdots\cdots(20)$$

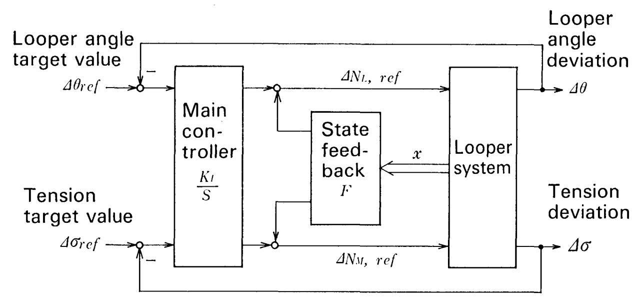

Fig. 6. Block diagram of optimal multivariable control.

and inserted into Eq. (18), the manipulated vector u is obtained as

$$u=-R^{-1}B^TK_{21}\int_{t_0}^{t}(y-y_R)dt-R^{-1}B^TK_{22}x+Z_{(t_0)}. \quad \cdots\cdots(21)$$

The main controller gain matrix K_I and state feedback gain matrix F obtained from Eqs. (14) and (21) can be expressed as

$$K_I=R^{-1}B^TK_{21},\ F=-R^{-1}B^TK_{22}. \quad \cdots\cdots(22)$$

2. Selection of State Feedback Term

A simulation study was performed to determine the effect of the state feedback variable of the looper system indicated in Fig. 7, or each element of Eq. (11), on the control characteristics based on the movement of the pole position when the feedback gain is altered.

For the simulation, a dynamic simulator of a six-stand hot strip finishing mill was used. The optimal multivariable control was applied to the looper between stands F4 and F5 in this simulation. The looper angle reference was changed to $+5°$ from its initial reference value, and the tension reference was changed to $+4.9$ MPa from its initial reference value at a time 4.5 s. The resulting values of the various state feedback variables were compared. The results of this simulation are indicated in Fig. 7.

The results of simulation showed the following three points:

(1) The state feedback variables that greatly affect the speed correction value of the main motor are the tension and looper angle.

(2) The state feedback variables that greatly affect the speed correction value of the looper motor are also the looper angle and tension.

(3) The feedback quantities of the armature current and speed of the main motor ΔI_M, ΔN_M and the armature current of the looper motor ΔI_L are small.

Next, the change in the pole position on adjustment of each of the state feedback gains was investigated. The change in gain was set at 0×, 0.5×, 2× and 4× of the reference gains employed in the simulation. A sample of the calculation results is given in Fig. 8. Based on these results, further conclusions were obtained:

(4) Pole position is greatly affected by the change in looper angle feedback gain. Thus, the influence of the looper angle on closed-loop characteristics is high. Tension feedback gain also exhibits nearly the same influence on pole position and is thus a major factor affecting closed-loop characteristics as well.

(5) The effect of feedback gain from the armature current of the looper motor is minimal. The pole position does not change even if the gain is varied. This holds true for the main motor speed and the current as well.

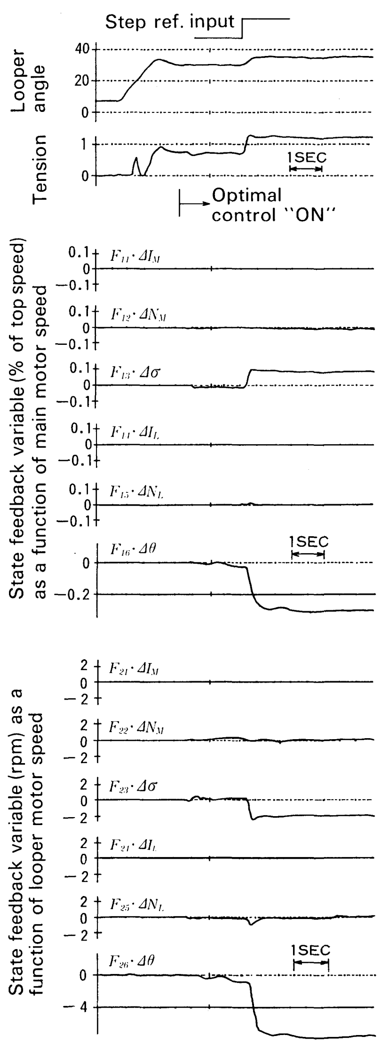

Fig. 7. Simulation results (feedback term).

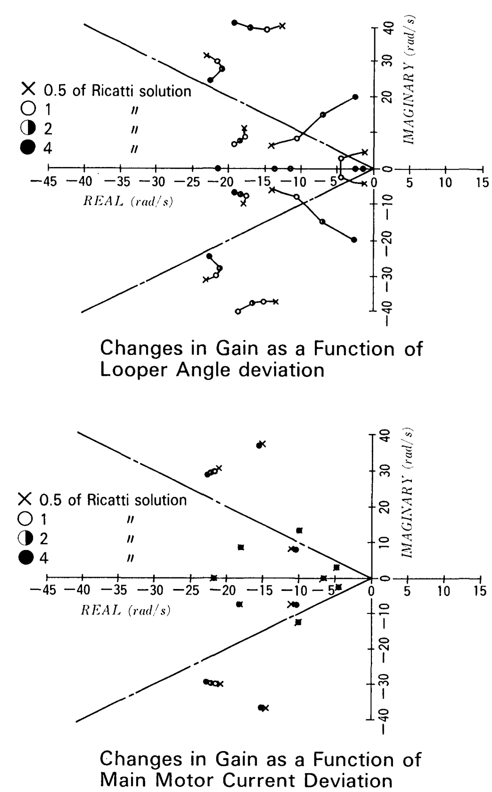

Fig. 8. Pole position change.

(6) The feedback value of the looper motor speed has an intermediate contribution between (4) and (5).

These results are consistent with the simulation results. It is thus clear that the major state feedback variables are tension, looper angle and looper motor speed.

V. Dynamic Simulation of Control Performance

Dynamic simulation was performed to evaluate the control performance before application of the looper optimal multivariable control to a production mill.

Two dynamic simulations were performed, one with the conventional control of all loopers and the other with the optimal multivariable control of all loopers. Figures 9(a) and 9(b) indicate the results of the conventional control and the optimal multivariable control, respectively. Under the conventional control, the tension and looper angle fluctuate due to the temperature drop near by the part of a skid mark. No significant fluctuation arises with the optimal multivariable control.

As indicated in Fig. 9, the optimal multivariable control can reduce the tension and looper angle fluctuations to a low level.

VI. Application to Actual Mill

1. Control System

The configuration of the system for looper optimal multivariable control is illustrated in Fig. 10. The looper optimal multivariable control is achieved with a programmable controller. Input and output of the accumulated data and manipulated variables are performed through a high-speed optimal transmission unit.

2. On-line Operation

An example of on-line results is given in Fig. 11. The three coils indicated in the figure were processed under the same rolling conditions. Only the method of looper control was varied. All of the coils are particularly subject to large disturbances such as fluctuations in the temperature.

Figure 11 clearly indicates that, in the conventional control, both tension and looper angle undergo large fluctuations. In the non-interactive control the fluctuation in the looper angle is smallest, although the fluctuation in tension is rather high. In the case of optimal multivariable control, however, the fluctuation in tension is smallest and a slight fluctuation in

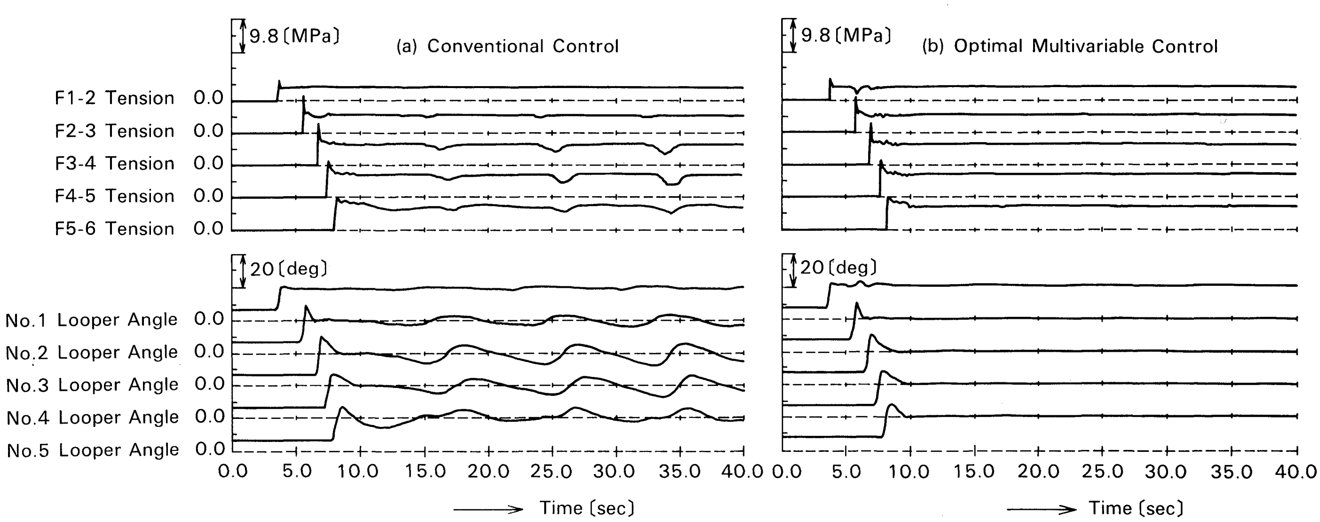

Fig. 9. Simulation results (performance test).

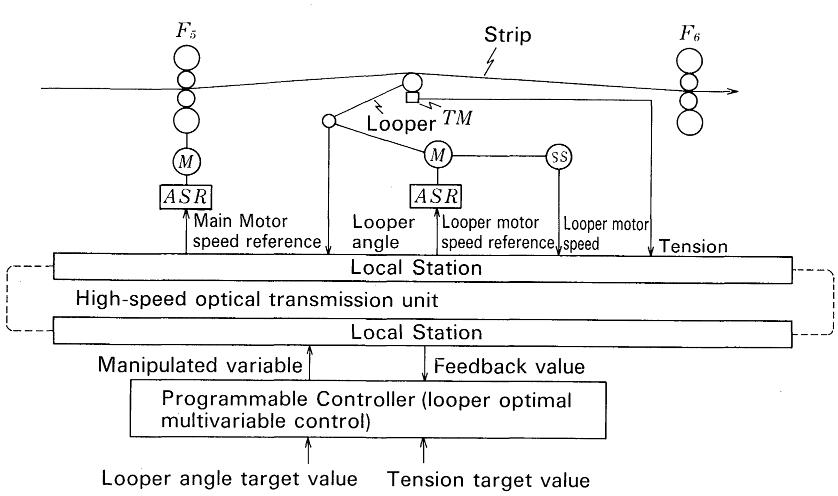

ASR: Automatic speed regulator
TM: Tension meter
M: Motor
SS: Speed sensor

Fig. 10.
System configuration of looper optimal multivariable control.

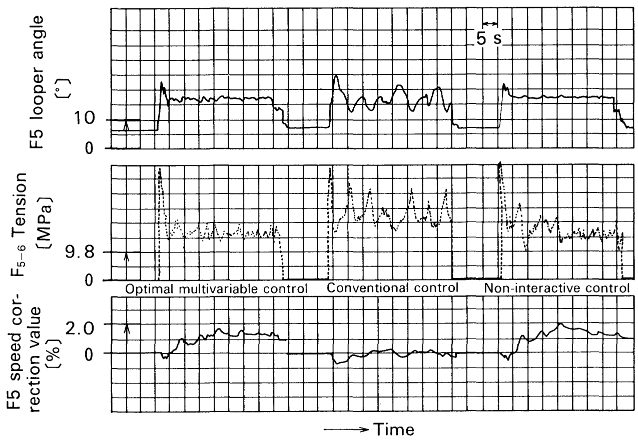

Fig. 11. On-line results.

looper angle leads to a significant improvement in tension fluctuation. Though in this method the looper angle fluctuation is greater than in the non-interactive control, it is still within the limits allowable in operation.

The standard deviation of the looper angle and tension is shown in Fig. 12. The improvement in tension fluctuations due to the optimal multivariable control is evident in Fig. 12. The tension fluctuation in the looper non-interactive control is 83 % of those of the conventional control. The tension fluctuation in the looper optimal multivariable control is 45 % of those of the conventional control. In addition, the tension fluctuation in the looper optimal multivariable control is 24 % of those of the conventional control. This is nearly the same as for the non-interactive control.

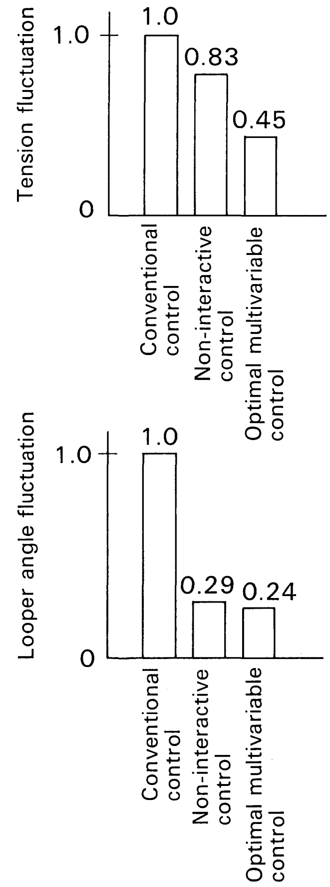

Fig. 12. Standard deviation of tension and looper angle.

VII. Conclusion

Investigation of an integral-type optimal regulator for the optimal multivariable control and subsequent application to a production mill have proved that the present control system is advantageous over the conventional method and the non-interactive method in terms of tension control accuracy and looper angle control accuracy.

The results can be summarized as follows:

(1) The looper optimal multivariable control system based on an optimal regulator theory has been developed.

(2) The looper optimal multivariable control is effective in increasing the stability of tension and looper angle. In turn, the response time of automatic gage control can be improved.

(3) As a result of the evaluation of various state feedback terms through simulation and of effects on pole position, it is found that the contributing terms to simplification of the control system are to selected only. This allows a programmable controller to be employed for the optimal multivariable control.

REFERENCES

1) S. Nishibayashi, S. Hatae, M. Haga and K. Hirase: *Iron Steel Eng.*, **63** (1986), No. 10, 49.
2) J. C. Price: *IEEE Trans. Ind. Appl.*, (1973), Sep./Oct., 556.
3) Y. Anbe, H. Watanabe, K. Kobayashi and T. Moritaka: *Trans. Inst. Electr. Eng. Jpn.* **107-c** (1987), 857.
4) K. Sekiguchi, Y. Seki, Y. Anbe, K. Fukushima, Y. Tuji and S. Ueno: *Trans. Inst. Electr. Eng. Jpn.*, **108-c** (1988), No. 1, 31.